JOC Article

Proton as the Simplest of All Catalysts for [2 + 2] Cycloadditions: DFT Study of Acid-Catalyzed Imine Metathesis

Matthew C. Burland,[†] Tara Y. Meyer,[‡] and Mu-Hyun Baik*,[†]

Department of Chemistry and School of Informatics, Indiana University, Bloomington, Indiana 47405, and Department of Chemistry, University of Pittsburgh, Pittsburgh, Pennsylvania 15260

mbaik@indiana.edu

Received May 3, 2004

The mechanism of imine metathesis was studied as a prototype reaction for the impact that heteroatom substitution has on thermally forbidden [2 + 2] addition reactions using high-level density functional theory in combination with a continuum solvation model. The intuitively expected high activation barriers were confirmed for *N*-alkyl- and *N*-aryl-substituted imine reactants with transition state free energies of 78.8 and 68.5 kcal/mol, respectively, in benzene. The computed reaction energy profiles were analyzed to discover possible strategies for lowering the transition state energy. Protonation of the imine nitrogen was proposed as a possible catalytic route and was explicitly modeled. The computed reaction energy profile shows that protonation of one of the imine reactants has an enormous effect on the overall rate of metathesis and lowers the activation barrier by as much as 37.3 and 30.6 kcal/mol for the *N*-alkyl and *N*-aryl reactants, respectively. These results suggest that acid-catalyzed imine metathesis should be amenable at elevated temperatures. Furthermore, the protonation of both reactants of the metathesis reaction is predicted to be not productive owing to electrostatic repulsion of the reactants, thus suggesting that there should be an optimum pH for the catalytic turnover. A detailed analysis of the catalytic mechanism is presented, and the primary driving force for the catalysis is identified. Upon protonation of the imine nitrogen, the key [2 + 2]-addition step becomes asynchronous and one of the two intermolecular N−C bonds is formed before traversing the transition state, resulting in a substantial net decrease of the overall energy requirement. The general applicability of this intuitively understandable mechanism for designing structural features for lowering the energy of transition state structures is explored.

Introduction

Olefin metathesis is an important and versatile tool for both synthetic organic[1−3] and inorganic chemistry.[4] This reaction involving the exchange of $=CR_2$ groups between two olefins to form new olefinic products has found great utility for small molecule synthesis especially in the form of ring-closing metathesis (RCM).[5,6] The olefin metathesis methodology has also provided access to some novel polymerization processes via ring-opening metathesis polymerization (ROMP).[7−9] For carrying out olefin metathesis reactions efficiently, transition metal catalysts are usually employed, with the most effective complexes being alkylidene- or benzylidene-based carbene systems that contain a metal−carbon double bond.[10,11] The generally accepted mechanism for the transition-metal-catalyzed metathesis reaction is the [2 + 2] addition/elimination mechanism proposed by Chauvin (Scheme 1).[12] A [2 + 2] addition of the olefin double bond to the metal−carbon double bond of the catalyst affords a metallocyclobutane intermediate, which concomitantly retrocyclizes either nonproductively, yielding starting material, or productively to produce a new olefin and a new alkylidene. The newly produced alkylidene can reenter the catalytic cycle and react with more olefin to give an overall reaction of CR_2 exchange between olefins. The catalyst acts as a CR_2 group shuttle between olefins since they cannot react together directly (vide infra). In the absence of a thermodynamic driving force in favor of

SCHEME 1

[†] Indiana University.
[‡] University of Pittsburgh.

(1) Grubbs, R. H.; S., C. *Tetrahedron* **1998**, *54*, 4413.
(2) Ivin, K. J. *J. Mol. Catal. A* **1998**, *133*, 1.
(3) Schrock, R. R. *Tetrahedron* **1999**, *55*, 8141.
(4) Johnson, L. K.; Virgil, S. C.; Grubbs, R. H. *J. Am. Chem. Soc.* **1990**, *112*, 5384.
(5) Armstrong, S. K. *J. Chem. Soc., Perkin Trans. 1* **1998**, 371.
(6) Maier, M. E. *Angew. Chem., Int. Ed.* **2000**, *39*, 2073.
(7) Grubbs, R. H.; Tumas, W. *Science* **1989**, *243*, 907.
(8) Schrock, R. R. *Acc. Chem. Res.* **1990**, *23*, 158.
(9) Amass, A. J. In *New Methods of Polymer Synthesis*; Ebdon, J. R., Ed.; Chapman and Hall: New York, 1991; p 76.
(10) Trnka, T. M.; Grubbs, R. H. *Acc. Chem. Res.* **2001**, *34*, 18.
(11) Schrock, R. R.; Hoveyda, A. H. *Angew. Chem., Int. Ed.* **2003**, *42*, 4592.
(12) Hérisson, J.-L.; Chauvin, Y. *Macromol. Chem.* **1970**, *141*, 161.

10.1021/jo049250e CCC: $27.50
Published on Web 08/20/2004

one set of olefin products over another, the reaction will yield a statistical mixture of all possible products. Therefore, the key to making the metathesis reaction useful lies in choosing the reactants such that at least one product will be energetically downhill enough to drive the overall reaction to completion.

Although olefin metathesis has garnered a great deal of interest in the organometallic chemistry community, the catalytic metathesis of carbon−heteroatom double bonds has seen little attention to date. Recently, several new systems for the catalytic metathesis of C=N bonds in imines have been reported,[13−27] which open up potential new avenues for synthesis. For exploiting imine metathesis as a novel synthetic tool, it is important to understand the mechanism in greater detail than currently available. In addition, the reaction is very interesting from a more fundamental mechanistic perspective. First, the absence of a transition metal simplifies the electronic structure analysis and gives access to a more intuitive understanding of the features that govern the thermodynamics and kinetics of metathesis-type reactions in general. Second, imine and olefin substrates are isoelectronic and thus allow a direct comparison of the mechanistic details. The observation of thermally allowed, albeit acid-catalyzed, [2 + 2] addition when imines are used[28] is also intriguing in view of the fact that the analogous olefin reaction is only allowed photochemically.[29,30] A truly rational and strategic approach to catalyst design is in part difficult because a detailed understanding of the electronic and mechanistic features that govern the metathesis on an atomic level is not available. In this study, we employ computational electronic structure methods to derive such an understanding for the imine metathesis reaction as a prototype reaction involving Chauvin-type mechanisms. To better serve as a realistic guide for future experimental work, we make use of the reactants PhCH=NPr, PhCH=N(*p*-tolyl), and (*p*-tolyl)CH=NPh, which have previously been examined[14] or are likely to be easily accessible.

Computational Details

All calculations were carried out using density functional theory as implemented in the Jaguar 5.5 suite[31] of ab initio quantum chemistry programs and the Amsterdam Density Functional 2003.02 package (ADF).[32] Geometries were optimized using Jaguar and the B3LYP functional[33,34] with the 6-31G** basis set. Although this basis set has been shown to be useful for geometry optimizations, the actual energies have frequently been observed to be not sufficiently accurate. Thus, the energies were reevaluated by additional single point calculations at each optimized geometry using Dunning's[35] correlation consistent triple-ζ basis set cc-pVTZ(-f) with the standard double set of polarization functions. Solvation corrections were added using a self-consistent reaction field (SCRF) approach,[36−38] by numerically solving the Poisson−Boltzmann equation.[39,40] These calculations were carried out at the gas-phase geometry using the 6-31G** basis and employing a dielectric constant of $\epsilon = 2.284$ for benzene. Whereas the accurate computation of absolute solvation energies remains a challenge and potentially requires careful inspection of the empirical parameters, the differential solvation energy is expected to be less sensitive owing to significant error cancellation when the same empirical parameters are used. Thus, the differential solvation corrections are most likely more reliable than the absolute energies of solvation.[41]

To locate transition states, the potential energy surface was first explored approximately using the linear synchronous transit method (LST),[42] followed by a quadratic synchronous transit (QST)[43] search using the LST transition state as an initial guess. In QST, the initial part of the transition state search is restricted to a circular curve connecting the reactant, initial transition state guess, and the product followed by a search along the Hessian eigenvector that is most similar to the tangent of this curve. Vibrational frequency calculation results based on analytical second derivatives at the B3LYP/6-31G** level of theory were used to confirm proper convergence to local minima or local maxima of the potential energy surface. Zero-point-energy (ZPE) and entropy corrections were derived using unscaled frequencies. We applied standard approximations to evaluate the partition functions.

Additional single point calculations on the Jaguar-optimized structures were carried out using ADF to obtain fragment wave functions and to calculate energy decompositions according to the extended transition state (ETS) theory derived and implemented in ADF by Ziegler and Rauk.[44,45] In these calculations, a double-ζ STO basis set is utilized, with one set of polarization functions as provided in the ADF package (Basis Set DZ - frozen core), together with the BLYP functional.[34,46]

For obtaining physically meaningful and realistic energies of reaction profiles it is in general important to correct for

(13) Burland, M. C.; Pontz, T. W.; Meyer, T. Y. *Organometallics* **2002**, *21*, 1933.
(14) Burland, M. C.; Meyer, T. Y. *Inorg. Chem.* **2003**, *42*, 3438.
(15) Cantrell, G. K.; Meyer, T. Y. *Organometallics* **1997**, *16*, 5381.
(16) Cantrell, G. K.; Meyer, T. Y. *J. Am. Chem. Soc.* **1998**, *120*, 8035.
(17) Meyer, K. E.; Walsh, P. J.; Bergman, R. G. *J. Am. Chem. Soc.* **1994**, *116*, 2669.
(18) Meyer, K. E.; Walsh, P. J.; Bergman, R. G. *J. Am. Chem. Soc.* **1995**, *117*, 974.
(19) Krska, S. W.; Zuckerman, R. L.; Bergman, R. G. *J. Am. Chem. Soc.* **1998**, *120*, 11828.
(20) Zuckerman, R. L.; Krska, S. W.; Bergman, R. G. *J. Am. Chem. Soc.* **2000**, *122*, 751.
(21) McInnes, J. M.; Mountford, P. *J. Chem. Soc., Chem. Commun.* **1998**, 1669.
(22) Mountford, P. *J. Chem. Soc., Chem. Commun.* **1997**, 2127.
(23) Royo, P.; Sánchez-Nieves, J. *J. Organomet. Chem.* **2000**, *597*, 61.
(24) Birdwhistell, K. R.; Lanza, J.; Pasos, J. *J. Organomet. Chem.* **1999**, *584*, 200.
(25) Weiss, K.; Kindl, P. *Angew. Chem., Int. Ed. Engl.* **1984**, *23*, 629.
(26) Bruno, J. W.; Li, X. J. *Organometallics* **2000**, *19*, 4672.
(27) Buhl, M. *Chem. Eur. J.* **1999**, *5*, 3514.
(28) Tóth, G.; Pintér, I.; Messmer, A. *Tetrahedron Lett.* **1974**, *15*, 735.
(29) Dilling, W. L. *Chem. Rev.* **1966**, *66*, 373.
(30) Mehta, G.; Srikrishna, A.; Reddy, A. V.; Nair, M. S. *Tetrahedron* **1981**, *37*, 4543.
(31) *Jaguar*, 5.5 ed.; Schrödinger, L.L.C.: Portland, OR, 1991−2003.
(32) Velde, G. T.; Bickelhaupt, F. M.; Baerends, E. J.; Guerra, C. F.; Van Gisbergen, S. J. A.; Snijders, J. G.; Ziegler, T. J. *Comput. Chem.* **2001**, *22*, 931.
(33) Becke, A. D. *J. Chem. Phys.* **1993**, *98*, 5648.
(34) Lee, C. T.; Yang, W. T.; Parr, R. G. *Phys. Rev. B* **1988**, *37*, 785.
(35) Dunning, T. H. *J. Chem. Phys.* **1989**, *90*, 1007.
(36) Cramer, C. J.; Truhlar, D. G. *Chem. Rev.* **1999**, *99*, 2161.
(37) Cramer, C. J.; Truhlar, D. G. *Structure and Reactivity in Aqueous Solution*; ACS Symposium Series 568; American Chemical Society: Washington, DC, 1994.
(38) Tomasi, J.; Persico, M. *Chem. Rev.* **1994**, *94*, 2027.
(39) Marten, B.; Kim, K.; Cortis, C.; Friesner, R. A.; Murphy, R. B.; Ringnalda, M. N.; Sitkoff, D.; Honig, B. *J. Phys. Chem.* **1996**, *100*, 11775.
(40) Tannor, D. J.; Marten, B.; Murphy, R. B.; Friesner, R. A.; Sitkoff, D.; Nicholls, A.; Ringnalda, M. N.; Goddard, W. A. I.; Honig, B. *J. Am. Chem. Soc.* **1994**, *116*, 11875.
(41) Baik, M.-H.; Friesner, R. A. *J. Phys. Chem. A* **2002**, *106*, 7407.
(42) Halgren, T. A.; Lipscomb, W. N. *Chem. Phys. Lett.* **1977**, *49*, 225.
(43) Peng, C. Y.; Schlegel, H. B. *Isr. J. Chem.* **1993**, *33*, 449.
(44) Ziegler, T.; Rauk, A. *Theor. Chim. Acta* **1977**, *46*, 1.
(45) Ziegler, T.; Rauk, A. *Inorg. Chem.* **1979**, *18*, 1755.
(46) Becke, A. D. *Phys. Rev. A* **1988**, *38*, 3098.

entropy and vibrational zero point effects, thus considering the free energies rather than the electronic energies as computed in standard self-consistent-field (SCF) calculations. However, the uncorrected electronic energies are usually the most interesting terms because they are the direct reporters of electronic reorganizations that constitute the main driving forces of chemical reactions that form the basis for intuitive chemical concepts. Thus, we pay special attention to the electronic energies E(SCF), which are the uncorrected SCF energies. Adding the vibrational zero-point energy (ZPE) to E(SCF) gives the physically meaningful gas-phase enthalpy *H*(GP), where thermal corrections to the enthalpy have been neglected. Adding entropy corrections at room temperature (298.15 K) that include vibrational entropies derived from the computed Hessians yields the free energy in the gas phase *G*(GP). Finally, the estimates for the free energy of solvation *G*(Solv) from the continuum models give access to the free energy in solution phase *G*(Sol). It is important to recognize that continuum models only deliver free energies of solvation and a partition of that energy into the enthalpic and entropic terms is intrinsically impossible.

Thus, combining reaction enthalpies ΔH(GP) with the differential solvation energy ΔG(Solv) gives a hybrid energy ΔH(Sol), which is rigorously not meaningful. However, because it captures two important terms of the total free energy that constitute most of the nontrivial differential reaction energies, we list this "solvation-corrected electronic energy". As observed elsewhere,[47] this hybrid energy is a fair approximation to the free energy of reaction in typical reaction energy profiles and is available at a fraction of the computational cost of a full-scale entropy-corrected energy requiring the explicit evaluation of the Hessian, which is only amenable for mid-sized models. Thus, one reason to consider the hybrid energy is to set the stage for future work on larger systems, where entropy corrections will not be available.

Orbital Analyses. In addition to knowing the energies at the different steps along the reaction pathway, it is highly desirable to understand the interactions between the reactants in a more detailed fashion. In this study, we used the fragment molecular orbital method in combination with the extended transition state (ETS) approach,[44,45] to decompose the computed interaction energies in conceptually intuitive terms. A review of this method and its application to inorganic problems is available.[48] We present only a brief overview of the ETS method below.

Rather than using total energy E on an absolute scale, a binding energy ΔE is defined in terms of molecular fragments by subtracting out the sum of fragment energies. The total binding energy is then conveniently partitioned into two main parts ΔE_{prep} and ΔE_{int}:

$$\Delta E = \Delta E_{\text{prep}} + \Delta E_{\text{int}} \tag{1}$$

In this equation, ΔE_{prep} is the energy required to change the relaxed geometry of the free fragment to that found in the molecule and ΔE_{int} is the interaction energy of the two fragments in the molecule. ΔE_{int} can be further decomposed, as indicated in eq 2, where ΔE_{Pauli} gives the repulsion force between two electrons of same spin trying to avoid the occupancy of the same spatial coordinates in accord with the Pauli principle:

$$\Delta E_{\text{int}} = \Delta E_{\text{Pauli}} + \Delta E_{\text{el-st}} + \Delta E_{\text{orb-int}} \tag{2}$$

The second term, $\Delta E_{\text{el-st}}$, gives the electrostatic interaction between the two fragments simply evaluated at a superimposed electron density distribution of the fragments. Finally, the fragment orbitals are allowed to relax and interact with each other, giving the orbital interaction term $\Delta E_{\text{orb-int.}}$ Only occupied orbitals contribute to the first two energy terms, whereas mixing of unoccupied orbitals and reorganization of occupied orbitals in the process of forming the final molecule determine the last term.

Results and Discussion

General Considerations. The first part of the olefin metathesis reaction according to the Chavin mechanism is a [2 + 2] cyclization leading to the four-membered ring intermediate. Woodward−Hoffmann rules[49,50] predict this reaction to be not allowed thermally owing to the mismatch in frontier orbital symmetry, suggesting very high activation barriers under standard conditions. Similarly, the second step of the metathesis reaction, i.e., the ring-opening process to give the final product, is thermally forbidden. Consequently, the four-membered ring intermediate is expected to be trapped in a steep potential well. Our computational exploration of this hypothetical mechanistic scenario confirmed that the self-metathesis reaction of an asymmetrically functionalized olefin PhCH=CH(*p*-tolyl) is highly unfavorable. The free energy of activation for the formation of the intermediate was estimated to be ~66 kcal/mol,[51] suggesting that this reaction is practically impossible at reasonable conditions. Both for a detailed understanding of metathesis reactions in general and to formulate strategic approaches to rational design of metathesis catalysts, it is therefore important to discover means of overcoming the intrinsic barrier of electronic reorganization by functionalizing the olefin skeleton.

Imine Metathesis. One functionalization strategy is to replace half of the olefinic monomer, the $=CR_2$ moiety, with an isolobal entity such as an imine group, =NR. The higher electronegativity of N is expected to shift the nitrogen p-orbitals that participate in π-bonding to lower energies, thus causing a nonsymmetric distortion of the π and π^* orbitals such that the nitrogen character is increased in the occupied π orbital, whereas the π^* orbital is expected to be dominated by carbon p-orbital character. A nonsymmetric electron density distribution across the double bond is therefore an obvious result, which should in principle favor the [2 + 2] addition type of reaction both by allowing dipole−dipole driven precoordination of the reactants and biasing the heterolytic double-bond cleavage by localizing the electron density on the nitrogen atoms. Electronically, this substitution allows for breaking the orbital symmetry of the olefinic unit to make the [2 + 2] cyclization thermally allowed. The imine functionality is also interesting because of its potential ability to form a σ-bond with an electrophile utilizing the N-lone pair without having to lose the double-bond character to do so.

Modeling chemical reactions where weak interactions between different reactants are important is challenging in general and is particularly difficult for Density Functional Theory methods. In the course of the metathesis reaction, weak interactions gives rise to the formation of precoordination complexes, the energies of which are

(47) Tang, L. H.; Papish, E. T.; Abramo, G. P.; Norton, J. R.; Baik, M. H.; Friesner, R. A.; Rappe, A. *J. Am. Chem. Soc.* **2003**, *125*, 10093.
(48) Frenking, G.; Fröhlich, N. *Chem. Rev.* **2000**, *100*, 717.
(49) Woodward, R. B.; Hoffmann, R. *Angew. Chem., Int. Ed. Engl.* **1969**, *8*, 781.
(50) Fukui, K. *Acc. Chem. Res.* **1971**, *4*, 57.
(51) See Supporting Information for details.

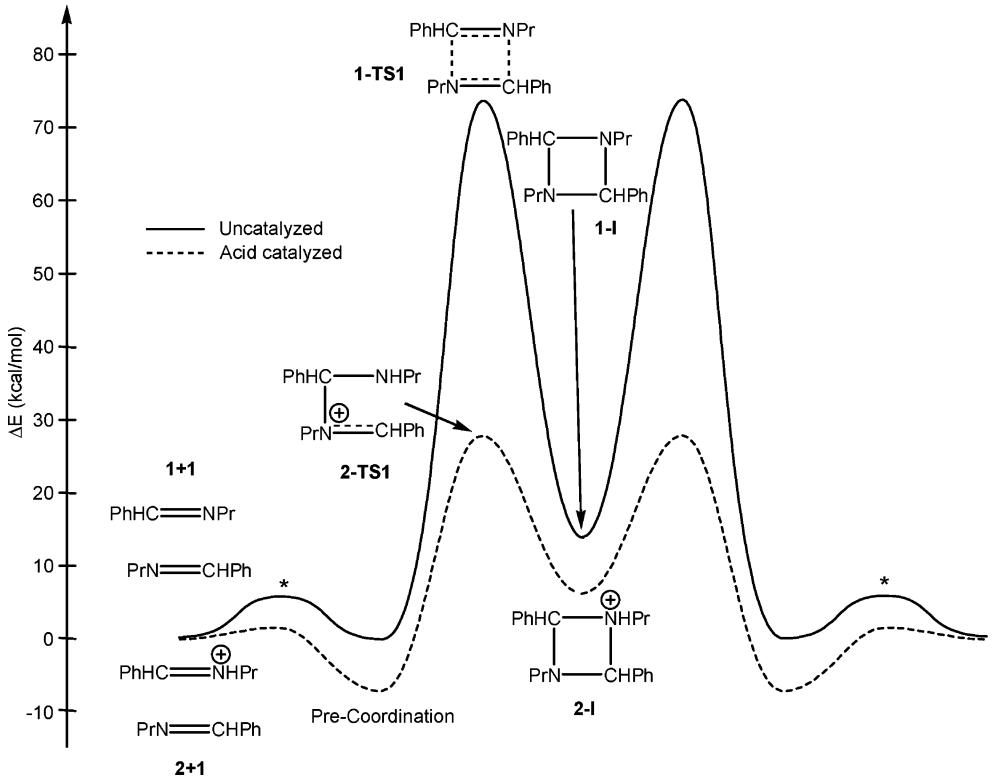

FIGURE 1. Reaction energy profile of the imine metathesis reaction. Uncorrected electronic energies, E(SCF), are used. (*) Transition states to the precoordination species were not found and are included only for illustration.

SCHEME 2

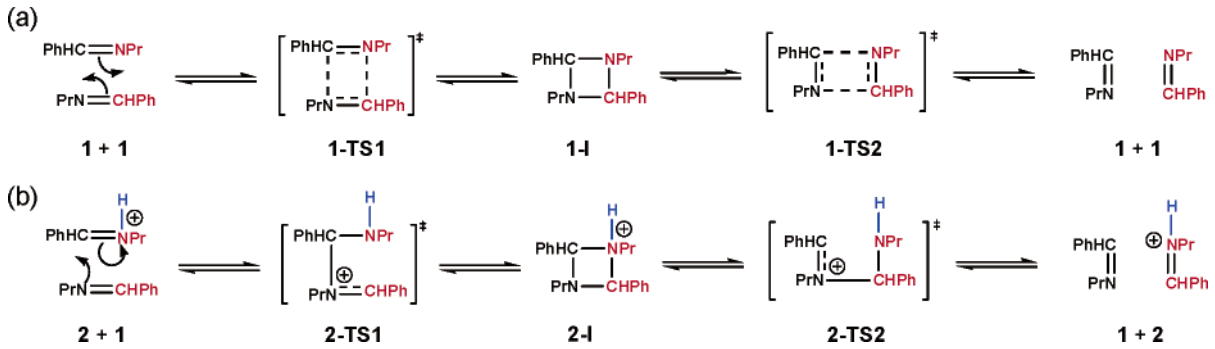

potentially not computed to a sufficient accuracy by DFT methods. The deficiency of DFT methods for van der Waals complexes has readily been shown in the literature.[52−54] Therefore, it is advisable to carefully benchmark the computationally efficient DFT calculations with a correlated ab initio method, such as the second order Møller−Plesset perturbation theory methods (MP2),[55] by comparatively inspecting the structures and energies of selected stationary points of the potential energy surface. Such a study that confirmed the general applicability of DFT for our specific modeling problem is presented in Supporting Information. Our benchmark calculations on small model systems indicate that the DFT results are fully reliable for the present purposes, although the DFT calculations did tend to underestimate the absolute barrier heights by about 20% and should thus be considered lower limits for the activation energies.

Noncatalyzed Imine Metathesis. The calculated imine metathesis mechanism for *N*-alkyl imine PhHC═NPr, **1**, is shown in Scheme 2a, and the corresponding reaction energy profile is plotted in Figure 1. The analogous reaction of the *N*-aryl imine PhHC═NTol + TolHC═NPh, **3** + **4**, is illustrated in Scheme 3a, and the corresponding reaction energy profile is given in Figure 2. Solution phase activation free energies, $\Delta G^{\ddagger}$(sol), of 78.8 and 68.5 kcal/mol for the *N*-alkyl and *N*-aryl cases, respectively, indicate that replacing ═CR_2 functionality by ═NR is not sufficient to make any notable changes to the [2 + 2] cyclization reaction. Neglect of the ZPE, entropy, and solvation corrections yields the purely electronic activation energies ($\Delta E^{\ddagger}$(SCF)),which amounts to 73.7 and 65.9 kcal/mol, respectively, confirming that the key to conceptually understanding the energy content

(52) Wu, Q.; Yang, W. T. *J. Chem. Phys.* **2002**, *116*, 515.
(53) Perezjorda, J. M.; Becke, A. D. *Chem. Phys. Lett.* **1995**, *233*, 134.
(54) Kristyan, S.; Pulay, P. *Chem. Phys. Lett.* **1994**, *229*, 175.
(55) Møller, C.; Plesset, M. S. *Phys. Rev.* **1934**, *46*, 618.

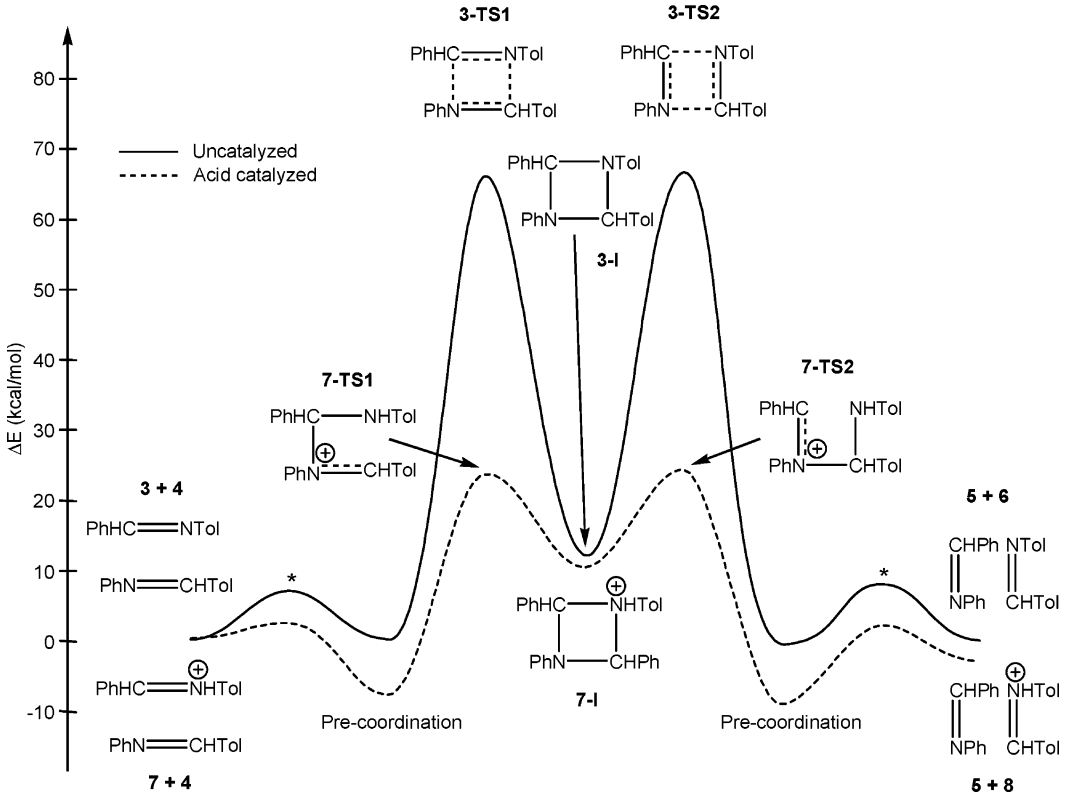

FIGURE 2. Reaction energy profile of *N*-aryl imine metathesis using E(SCF). (∗) Transition states to the precoordination species were not found and are included only for illustration.

SCHEME 3

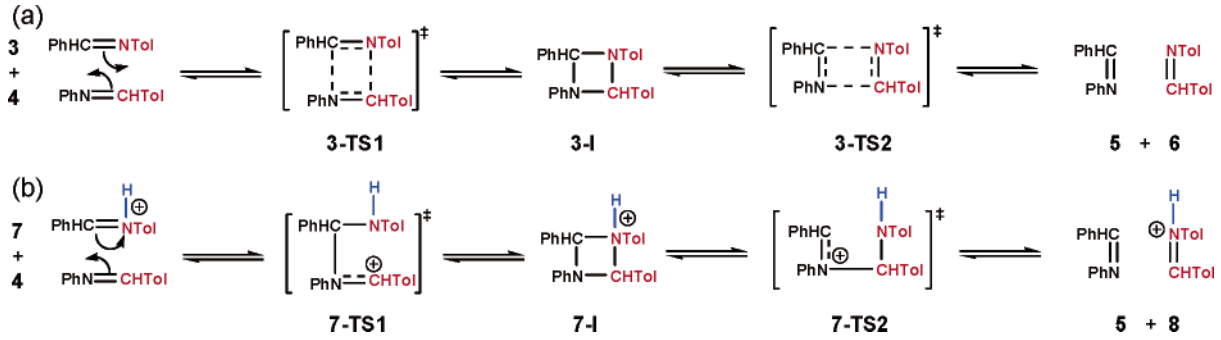

TABLE 1. Relative SCF Energy, Enthalpy, and Free Energy of Species Involved in the Reaction Depicted in Scheme 2a; All Energies Given in kcal/mol

	Δ*E*(SCF)	Δ*G*(Solv)	Δ*H*(Sol)	Δ*G*(Sol)
1 + **1**	0	−5.00	0	0
precoord	0.02	−3.46	1.56	10.52
1-TS1[a]	73.75	−2.40	76.35	89.32
1-I	13.84	−2.50	16.34	33.71

[a] Note that **1-TS2** is identical to **1-TS1** as a result of the degenerate nature of the reaction.

TABLE 2. Relative SCF Energy, Enthalpy, and Free Energy of Species Involved in the Reaction Depicted in Scheme 3a; All Energies Given in kcal/mol

	Δ*E*(SCF)	Δ*G*(Solv)	Δ*H*(Sol)	Δ*G*(Sol)
3 + **4**	0	−5.82	0	0
precoord **3** + **4**	2.31	−4.12	4.01	15.34
3-TS1	68.24	−4.67	69.39	83.84
3-I	13.97	−4.25	15.54	34.27
3-TS2	68.35	−4.72	69.45	84.09
precoord **5** + **6**	1.55	−4.22	3.15	15.91
5 + **6**	0.05	−6.88	−1.01	−1.23

of the metathesis reaction lies in electronic energy. Therefore Figures 1 and 2 show the electronic energies E(SCF), and the free energies are given in Supporting Information.

In accord with intuitive expectations, the intermediate, **2-I**, is a symmetric four-membered cycle with a N−C bond length of 1.48 Å (Figure 3b). The various possible orientations of substituents around the ring were considered in our calculations (see Supporting Information), and the lowest energy conformation is characterized by *syn* orientation of the functional groups directly connected to the carbon, whereas those attached to the nitrogen atom are *anti* to the carbon substituents. This structural motif is only possible when two *trans*-imines interact in a staggered orientation. Our calculations suggest that steric demands dictate this selective behav-

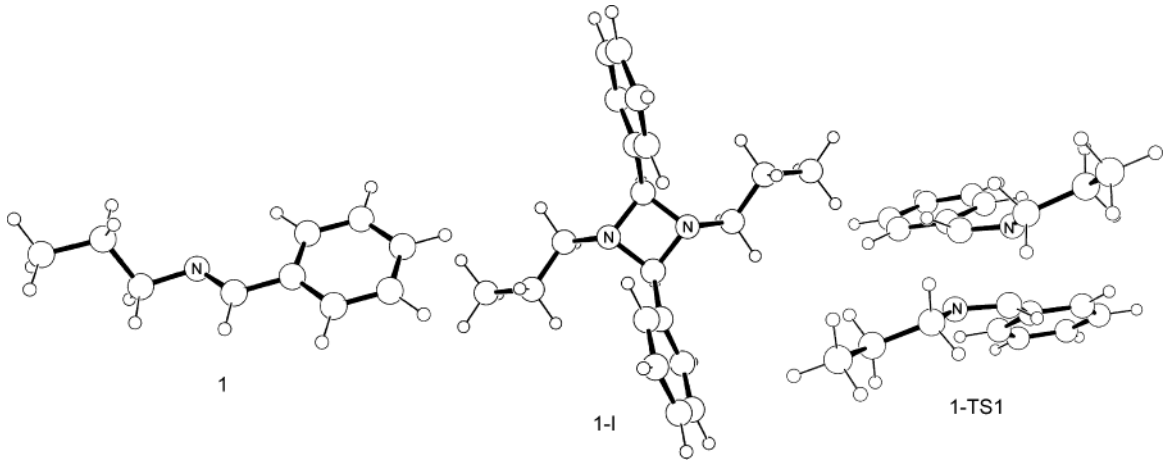

FIGURE 3. Optimized structures of the computed stationary point structures for the propyl-imine metathesis.

TABLE 3. Relative SCF Energy, Enthalpy, and Free Energy of Species Involved in the Reaction Depicted in Scheme 2b; All Energies Given in kcal/mol

	ΔE(SCF)	ΔG(Solv)	ΔH(Sol)	ΔG(Sol)
2 + **1**	0	−31.92	0	0
precoord	−7.06	−24.38	1.11	10.98
2-TS1[a]	28.04	−23.65	37.96	52.44
2-I	6.25	−24.73	16.83	31.60

[a] Note that **2-TS2** is identical to **2-TS1** as a result of the degenerate nature of the reaction.

TABLE 4. Relative SCF Energy, Enthalpy, and Free Energy of Species Involved in the Reaction Depicted in Scheme 3b; All Energies Given in kcal/mol

	ΔE(SCF)	ΔG(Solv)	ΔH(Sol)	ΔG(Sol)
7 + **4**	0	−30.13	0	0
precoord **7** + **4**	−6.36	−23.65	0.12	11.01
7-TS1	24.49	−22.49	32.13	48.89
7-I	10.24	−23.39	16.98	33.15
7-TS2	25.04	−22.66	32.51	48.25
precoord	−8.14	−23.46	−1.47	9.68
5 + **8**	−2.68	−30.27	−2.82	−1.73

ior both thermodynamically and kinetically, yielding the product with the least steric interaction between the substituents. Interestingly, the four-membered ring is not planar but shows a dihedral angle of 19.7°, which serves two purposes: (i) the steric interaction between the substituents around the four-membered ring is reduced, and (*ii*) the nitrogen atom becomes sp^3 hybridized and assumes a pseudotetrahedral geometry, where the lone-pair orbital occupies one of the main axis. If planarity of the ring is enforced, a structure is obtained that is calculated to be 5.5 kcal/mol higher in energy than the puckered ring. By enforcing planarity, the distance between the *ipso* carbons of the phenyl ring is reduced to 4.02 Å from 4.49 Å and the distance between the α-carbons of the propyl substituents is reduced to 4.03 Å from 4.47 Å in the puckered ring. These observations point to relief of the steric interaction between the substituents as an important driving force for the deformation from planarity. As expected, the nonplanarity of the ring, while reducing steric interaction between substituents, comes at the expense of reduced bond angles within the ring itself. The C−N−C angle is reduced to 88.4° from 89.4° and the N−C−N angle is reduced to 88.2° from 90.6° when the planar ring is allowed to relax to the puckered conformation.

An interesting feature of the metathesis reaction in general is the existence of a precoordination complex of the reactants. In this complex the two reactants interact mostly through electrostatic attraction.[56] In the case of the imine reactants, the complex is calculated to have a solution phase free energy 10−12 kcal/mol higher than that of the separate reactants, mostly as a result of loss of translation entropy and solvent-accessible surface area. Vibrational analyses of the precoordination complexes reveal that there are no imaginary frequencies and the complexes are true intermediate states. These readily accessible precoordinated reactant complexes act as stepping stones between the separated reactants and the transition states, thus lowering the activation barrier. If the model size is decreased by removing all functional groups (see Supporting Information), such intermediates could not be identified, suggesting that the substituents on the imines greatly enhance this interaction.[57]

A closer examination of the computed reaction mechanism reveals the reason for the high activation barrier: Both the olefin and imine metathesis reactions are concerted and synchronous. Figure 3c shows the calculated structure of the transition state **1-TS1**. The calculated transition state results from the interaction of two *trans*-imines. Extensive efforts to find any alternative transition states involving one *trans*- and one *cis*-imine or two *cis* imines failed to give stable structures. Thus, we concluded that transition state **1-TS1** is probably the lowest energy transition state. The C=N bond is elongated by 0.09 Å from the ground-state bond length of 1.27 Å to give 1.36 Å at the transition state, indicating that the double bond character is lost significantly. Meanwhile, the σ-bond between the two monomers is not formed to a notable extent, as confirmed by a Mayer[58]

(56) Clearly, van der Waals interactions will play a role in favoring the formation of the precoordination complex. However, DFT methods are well-known to completely neglect these attractive forces. Thus, our energy estimates must be taken as upper limits with the real values probably being 2−3 kcal/mol lower than computed.

(57) Note that we indicate transition states in Figures 1 and 3 that connect the free reactants with the precoordination complexes. These transition states cannot be located reliably using standard transition searches that samply the electronic energy surface, because they are highly dominated by translational entropy changes. A more detailed discussion of this problem can be found, e.g., in ref 65

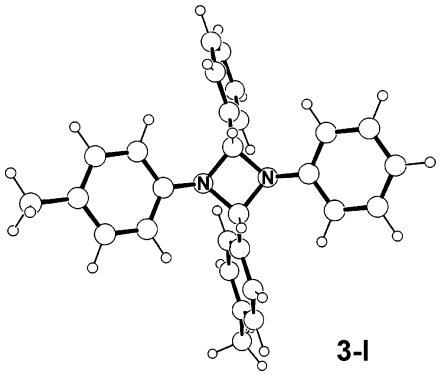

FIGURE 4. Optimized structures of *N*-aryl imine adduct **3-I**.

bond order of 0.35 and a N−C separation of 1.99 Å, converging to a typical distance observed before for similar transition state types.[59] As the double bond cleavage is an uphill process, whereas the formation of the new C−N single bond releases bond energy, and the transition state is dominated by double-bond breaking, the overall energy profile becomes prohibitively uphill.

Interestingly, the activation energy for the reaction involving *N*-aryl substituents is 7.8 kcal/mol lower than the activation energy for the *N*-alkyl-substituted case. At standard conditions, this energy difference corresponds to ∼10 orders of magnitude faster reaction for the *N*-aryl imines, thus predicting that an experimentally detectable difference of the reaction rates between the alkyl- and aryl-substituted systems is probable (vide infra). In the calculated structure for the adduct, **3-I**, in the *N*-aryl reaction (Figure 4) the aryl rings on the nitrogen atoms are orientated such that they are *pseudo*-coplanar with the four-membered ring. The four-membered ring is closer to planarity in the *N*-aryl case than in the *N*-alkyl case with a dihedral angle of only 14.3°. This increased planarity and the coplanar orientation of the *N*-aryl substituents suggests that resonance effects are present and lead to an additional stabilization of the intermediate. When examining the structure of the transition states for the *N*-aryl substituent (**3-TS1** and **3-TS2**) these resonance effects are already evident. At the transition state the *N*-aryl ring has already begun rotating away from planarity with the C═N bond, and this distortion promotes the formation of new single bonds. It is the introduction of these resonance effects at the transition state that is responsible for accelerating the *N*-aryl reaction relative to the *N*-alkyl case.

Our continuum solvation calculations suggest that solvation plays a notable but not decisive role. The solvation free energy of the *N*-alkyl imine monomer (**1**) is −2.5 kcal/mol, whereas −3.0 kcal/mol was computed for the aryl derivative (**3**). Intuitively, the solvation energy of **1-TS1** could be both higher or lower than the sum of the two reactant species, in each case providing an interesting insight to the underlying electronic driving force. If the electron densities of the two monomers do not distort significantly upon reaching the transition state, the mere fact that the solvent-accessible surface is reduced will give rise to a moderate loss of solvation energy. If, however, substantial reorganization of the electron density takes place resulting in a higher degreee of charge polarization, one would expect an increase of the solvation energy, which should be captured well by the continuum solvation model. Such a charge polarization is characteristic for heterolytic bond cleavages, where partial charge separation is the dominating effect. In the present case, the solvation energies of the transition states were −3.5 and −3.0 kcal/mol for the *N*-alkyl and *N*-aryl cases, respectively. Thus, upon formation of the transition state from the two fully separated monomers, 1.5 and 4.7 kcal/mol solvation energies are lost, respectively, indicating that there are no notable charge redistributions that are characteristic of heterolytic double bond cleavage processes.

In summary, it is clear that the substitution of the $=CR_2$ moiety with its isolobal analogue ═NR has a minimal effect of the activation energy of the metathesis reaction. The heteroatom-driven charge polarization effects and the possibility of involvement of the nitrogen lone pair do not appear to have the desired effect on the [2 + 2] addition/elimination mechanism.

Acid-Catalyzed Metathesis. Unlike in the case of olefin metathesis, the nitrogen lone-pair orbital of the imine group provides means of additional control of the reactivity by protonation (Schemes 2b and 3b). Protonation of one of the imine partners in the metathesis reaction leads to a dramatic reduction in the energy of the transition state relative to that of the uncatalyzed reaction. The free energy of activation in solution is lowered by 37.3 kcal/mol to give $\Delta G^{\ddagger}$(sol) = 41.5 for the *N*-alkyl system and by 30.6 kcal/mol to give $\Delta G^{\ddagger}$(sol) = 37.9 kcal/mol for the *N*-aryl system. The corresponding uncorrected electronic activation energies in gas phase $\Delta E^{\ddagger}$(SCF) are 35.1 and 30.9 kcal/mol (Figures 1 and 2). As observed above, the ZPE, entropy, and solvation terms give a constant shift and can be considered numerically significant but conceptually unimportant corrections.

These activation energies are low enough to make the reaction practical at modestly elevated temperatures. Interestingly, the difference in the energy of the adducts compared to that of the reactants is much less perturbed by protonation than the transition state. In the case of the *N*-alkyl-substituted imine, the electronic energy of the adduct (**2-I**) is 7.6 kcal/mol lower, while in the *N*-aryl-substituted imine (**7-I**) the energy is 3.7 kcal/mol lower than in the uncatalyzed case. When solvation and entropy corrections are taken into account, the differences become even less pronounced. Compared to the uncatalyzed reaction, the free energies in solution phase are 2.1 and 1.1 kcal/mol lower for the adduct in the acid-catalyzed *N*-alkyl and *N*-aryl systems, respectively. Given the dramatic changes observed in the transition state energies, this surprising invariance of the adduct energy means that the pK_a of the protonated imine functionality is not changing notably upon formation of the intermediate, which is an important requirement for the robustness of the catalytic reaction with respect to the second step. The robustness of the pK_a ensures that the proton remains attached to the *N*-moiety to mediate the ring-opening reaction.

The structure of the adduct in the acid-catalyzed reaction (**2-I**, Figure 5b) is very similar to the equivalent structure in the uncatalyzed reaction (**1-I**, Figure 3b).

(58) Mayer, I. *Int. J. Quantum Chem.* **1986**, *29*, 477.
(59) Houk, K. N.; Li, Y.; Evanseck, J. D. *Angew. Chem., Int. Ed. Engl.* **1992**, *31*, 682.

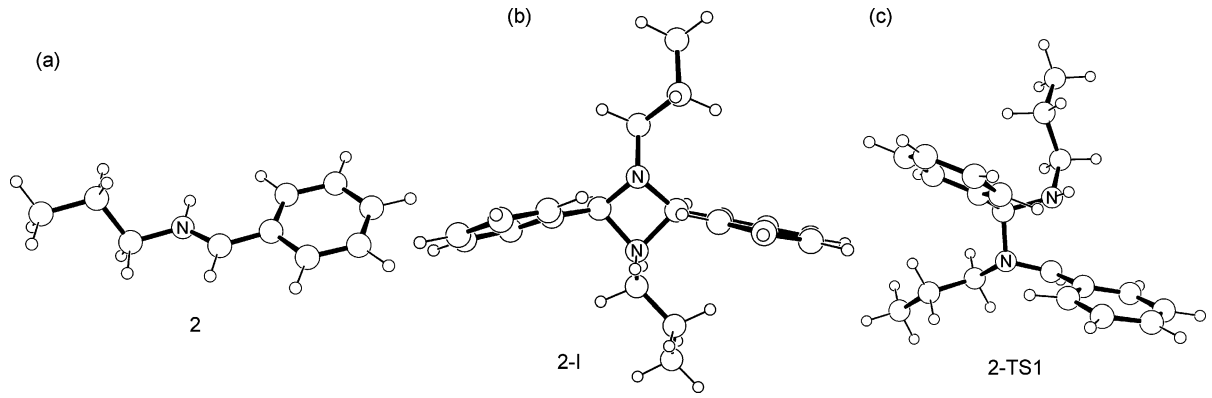

FIGURE 5. Optimized geometries of the key structures in the acid-catalyzed reaction.

Some of the symmetry present in **1-I** is lost in **2-I** as a result of the protonation of one of the two nitrogens. In **2-I**, the bonds to the protonated nitrogen are 1.55 Å, which is 0.08 Å longer than the 1.47 Å bonds to the unprotonated nitrogen in the same species. The adduct **2-I** is again nonplanar with a dihedral angle of 20.7°, which is 1.0° more than in **1-I**. Both of these effects, bond lengthening and nonplanarity, are best understood in terms of the loss of π-interactions around the four-membered ring due to the removal of the nitrogen p-orbital from π-subspace by protonation. The participation of the N-lone pair in the formation of the N−H σ-bond enforces the tetrahedral sp^3-configuration of the nitrogen atom.

Observing this influential effect, an alternative mechanism comes to mind that involves a different, more tightly bound precoordination complex. Attack of the imine nitrogen lone pair on the iminium carbon could give a strongly bound precoordination complex, instead of the loosely bound complex that we propose above. Such a species is observed indeed when the minimal size model is considered (see Supporting Information). Our calculations identified this alternative precoordination complex in our larger system as a stable structure, but it is theromodynamically not favorable when compared to the loosely bound complex. The free energetic preference amounts to 15.1 kcal/mol. The steric bulk of the substituents greatly disfavors a reaction route involving the initial attack on the nitrogen lone pair before the rate determining step is reached. Also interesting is the observation that trying to identify an alternative transition state starting from the lone-pair coordinated intermediate in this system leads only to the same transition state (**2-TS1**) that is seen when starting with the loosely bound intermediate. This convergence indicates that even if the reaction proceeds by attack of the lone pair, first the attacking imine must rotate around before the ring can close and therefore nothing is gained energetically by this route. The steric interaction could be reduced by reaction with a *cis*-imine; however, this structure is still disfavored by 7.1 kcal/mol compared to the loosely bound precoordination species. Moreover, the transition state for producing the ring closed intermediate **2-I** is an enormous 77.2 kcal/mol higher in energy than the lone-pair coordinated *cis*-imine adduct. Thus, this possible pathway involving the attack of the imine lone-pair to give an alternative intermediate is not constructive for the reaction.

The calculated transition state structure **2-TS1** (Figure 5c) is the lowest energy transition state found in this study. It is the transition state formed when a *trans*-imine and *trans*-iminium ion interact. Alternative conformations were probed, but they either minimized back to **2-TS1** or did not result in well-defined transition state structures.[60] By comparing **2-TS1** with **1-TS1**, the equivalent structure in the uncatalyzed reaction, the reason for the reduction in activation energy becomes easy to understand. The calculated structure for **2-TS1** is clearly asymmetric with the bond between the carbon of the iminium ion (**2**) and the nitrogen of the unprotonated imine (**1**) essentially fully formed at the transition state with a bond length of 1.49 Å, whereas the protonated nitrogen and the carbon of the unprotonated imine are separated by 2.19 Å, suggesting little or no interaction at the transition state. The C−N bond in the iminium ion (**2**) is elongated at the transition state by 0.19 Å from the ground-state bond length of 1.30 Å to give 1.49 Å, pointing to the presence of a single bond. In comparison, the C−N bond in imine **1** is elongated by only 0.11 Å to give 1.38 Å. These observations of the calculated structure of **2-TS1** show that one of the two bonds to be formed has already been formed and one of the double bonds to be broken has already been broken at the transition state. The reaction, while still concerted, has become *asynchronous*. This asynchronicity allows some of the energy spent on π-bond breaking to be regained by σ-bond formation before the transition state is reached. In contrast, the unprotonated case requires the investment of enough energy to almost completely break both π-bonds before any energy can be returned through σ-bond formation.

The energetics of the precoordination states has only a small differential effect on the overall reaction when the uncatalyzed and acid-catalyzed cases are compared. Although the electrostatic interaction in the precoordination state is greater in the acid-catalyzed system owing to the introduction of a net positive charge, this effect is offset by an increased loss of solvation when forming the precoordinated species. These effects counterbalance each other with the net result that the free energy of the precoordination state is qualitatively not significantly

(60) The electronic structure of 2-TS1 was calculated with the restricted spin formalism. As pointed out by a reviewer, it is possible that our computed configuration is only stable as a result of the restricted formalism. Thus, we have repeated the calculations in the unrestricted spin framework and found our proposed wave function to be stable.

changed when the proton is introduced. On the acid-catalyzed solution phase free energy surface, the formation of the precoordination complex from noninteracting reactants is 11.0 kcal/mol uphill for both the *N*-alkyl and *N*-aryl systems, whereas 10.5 and 12.6 kcal/mol, respectively, were computed for the uncatalyzed reaction. The more pronounced shift in the *N*-aryl system is primarily a consequence of a higher differential gain of entropy. We have explored this potentially interesting feature but did not find these effects enlightening for the main goal of this study and do not discuss it further.

Comparing the *N*-aryl imine reaction to the *N*-alkyl case it is notable that although the *N*-aryl imine reaction has an electronic activation energy that is 4.2 kcal/mol lower than that of the *N*-alkyl imine, the difference is not as dramatic as in the uncatalyzed reaction, where the relative electronic energies of the transition states differed by 7.5 kcal/mol. This observation is consistent with the conjecture that resonance effects involving the nitrogen substituent are important. When one of the nitrogen atoms in the *N*-aryl reactant is protonated it reduces the ability of the aryl ring to interact with the π system of the four-membered ring, as pointed out above. As a result, although the *N*-aryl reaction gains energetically from protonation, it does not gain as much as the *N*-alkyl system because it also loses some of the stabilizing resonance effects at the transition state. Thus, we expect that the catalytic mechanism outlined here will be more effective for *N*-alkyl systems than for *N*-aryl analogues, whereas the intrinsically higher reactivity of the *N*-aryl systems make it unlikely that this differential effect in catalytic activity will be experimentally detectable. These intuitively comprehensible trends will be attractive for the development of design strategies in the future.

Whereas protonation of one of the two imines involved in a metathesis reaction dramatically reduces the activation barrier, the reaction of two protonated imines together is an extremely high energy process mainly for two reasons. The electrostatic repulsion of two iminium cations would make the process energetically inaccessible. The equivalent structure to **2-I** when doubly protonated is calculated to be 93.8 kcal/mol higher in electronic energy than that of two separated iminium cations. In addition, protonation of both imine reactants gives rise to a symmetric transition state, and the formation of one C−N bond is no longer favored over that of the second C−N bond. Thus, the reaction becomes thermally forbidden. Consequently, the reaction rates in imine metathesis should accelerate with the addition of H^+, but adding more than 0.5 equiv of H^+ will cause the reaction to slow back down. Adding a full equivalent of acid should eliminate catalytic turnover. This effect has previously been reported in an experimental study.[28]

MO Analysis. Although the analysis of the computed reaction energy profiles presented above gives a thorough understanding of the acid-catalyzed imine metathesis mechanism as a perturbation of the putative uncatalyzed reaction, it is still unclear which electronic feature is the main driving force for decreasing the transition state energy. Specifically, the analysis presented so far does not unambiguously answer whether the catalytic mechanism can be generalized to, e.g., Lewis acids or whether there is a specific electronic feature that limits the validity of the discussed mechanism to a proton. To afford a more strategic and systematic design of metathesis catalyst in the future, a molecular orbital based concept of the acid catalysis is desirable. Figure 6 shows a partial MO diagram of the *N*-aryl-functionalized imine, depicting the most important molecular orbitals. Isosurface plots of some MOs depicted schematically in Figure 6 are shown in Figure 7. As can be expected, protonation of the imine nitrogen has only a very small effect on the shapes of the π- and π*-orbitals, since the empty s-orbital of the proton is orthogonal to these MOs, whereas the N-lone pair orbital, MO-50, is effectively removed from the frontier-orbital energy domain upon protonation by forming a N−H bonding σ-orbital, MO-28, with an orbital energy of −19.82 eV.

One important consequence of the positive charge that accompanies the proton is that it gives rise to a spherically symmetric electrostatic potential, which will lower both the σ- and π-orbital energies. Figure 6 illustrates the orbital energy changes to scale and shows that N-protonation forces the LUMO of the imine, a π*-orbital, to shift from its original energy of −1.60 to −6.61 eV in the iminium cation. The HOMO of the imine, a π-orbital at −5.75 eV, is therefore higher in energy than the LUMO of the iminium cation. Thus, intermolecular electron density donation from the HOMO of the imine to the LUMO of the iminium ion is electronically favorable, unlike in the original case, where it was energetically uphill by 4.15 eV in addition to being symmetry forbidden if a synchronous [2 + 2] addition is considered. Of course, the synchronous addition is still symmetry forbidden, but the electronic driving force is strong enough to make a new reaction pathway involving the asynchronous addition of the reactants energetically attractive.

The Ziegler−Rauk energy decomposition protocol[44,45] has become widely used in the recent past for quantitative analyses of relative energies between different intermediates of a chemical reaction.[48,61−66] Table 5 lists the energy decomposition results according to the Ziegler−Rauk method[67] for the four transition states **1-TS1**, **2-TS1**, **3-TS1**, and **7-TS1**, where the noninteracting reactants serve as reference points. Thus, the electronic energies of the transition states are decomposed relative to their respective reactants. The BLYP/double-ζ level of theory at the Jaguar-optimized geometries in ADF underestimates the absolute activation energies by approximately 10 kcal/mol.[68] However, all relative energies

(61) Baik, M. H.; Friesner, R. A.; Lippard, S. J. *J. Am. Chem. Soc.* **2003**, *125*, 14082.
(62) Cheng, R. J.; Chen, P. Y.; Lovell, T.; Liu, T. Q.; Noodleman, L.; Case, D. A. *J. Am. Chem. Soc.* **2003**, *125*, 6774.
(63) Frenking, G.; Wichmann, K.; Frohlich, N.; Loschen, C.; Lein, M.; Frunzke, J.; Rayon, V. M. *Coord. Chem. Rev.* **2003**, *238*, 55.
(64) Deubel, D. V. *J. Am. Chem. Soc.* **2002**, *124*, 5834.
(65) Baik, M. H.; Friesner, R. A.; Lippard, S. J. *J. Am. Chem. Soc.* **2002**, *124*, 4495.
(66) Ehlers, A. W.; Baerends, E. J.; Lammertsma, K. *J. Am. Chem. Soc.* **2002**, *124*, 2831.
(67) See Computational Details for an overview of the different terms.
(68) The use of B3LYP/6-31G** in geometry optimization also gave activation energies that were ∼4 kcal/mol too low (see Supporting Information). Thus, we contribute ∼5 kcal/mol of the disagreement to the smaller basis set and ∼5 kcal/mol to the use of BLYP instead of B3LYP. Note that the hybrid functional B3LYP requires Hartree−Fock calculations, which are not available in pure DFT packages, such as ADF.

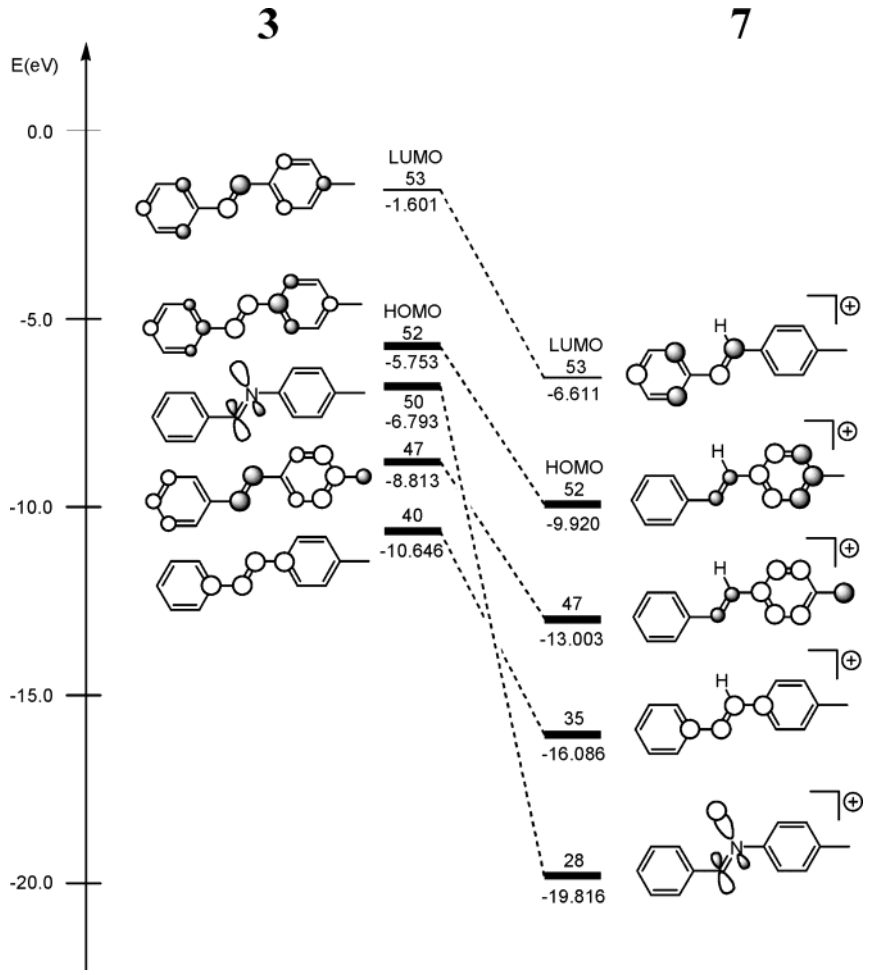

FIGURE 6. Schematic MO diagrams of the *N*-aryl imine and *N*-protonated iminium cation.

and differential effects upon protonation are reliably reproduced.

The noncatalyzed transition states **1-TS1** and **3-TS1** display typical characteristics of a highly inefficient [2 + 2] addition. The preparation energy E_{prep}, which is the energy required to distort the free reactants into a structure that they will adopt in the transition state, is moderately high with 0.64 eV (= 14.8 kcal/mol)[69] for each of the reactants. This is simply a measure for an early transition state with moderate structural distortions compared to the free reactants. The overall interaction between the two reactants is also repulsive, where the Pauli repulsion, i.e., the intermolecular electron−electron repulsion, is moderately high with 9.17 and 8.96 eV for the *N*-alkyl and *N*-aryl systems, respectively. The energetically favorable intermolecular electron−nucleus interaction between the fragments recovers 4.30 and 4.25 eV to give total nonorbital interaction energies of 4.87 and 4.72 eV, respectively. Orbital relaxations from these electronically strained fragment structures in the transition state adjust the total energy by −3.43 and −3.53 eV to give total interaction energies of 1.43 eV (= 33.0 kcal/mol) and 1.19 eV (= 27.4 kcal/mol) for the *N*-alkyl and *N*-aryl systems, respectively. If the preparation energies are taken into account, the final activation energy becomes 2.72 and 2.29 eV (= 62.7 and 52.8 kcal/mol), respectively. These results are in good agreement with the Jaguar values. Both the preparation and interaction energies favor the *N*-aryl species by 0.18 and 0.25 eV, respectively.

Upon protonation, the energy components change dramatically, which is expected given the substantial effects on activation energy discussed above. Comparing each of the energy components of the uncatalyzed with their acid-catalyzed analogues, it is clear that the lowering of the transition state energy is a consequence of stronger orbital interaction terms that increase from −3.43 and −3.53 eV in the uncatalyzed cases to −12.06 and −12.80 eV in the acid-catalyzed transition states. At the same time, the additional energy penalty owing to a more significant penetration of the fragment electron densities at the more compact transition state geometries amounts to 4.60 and 4.88 eV for the *N*-alkyl and *N*-aryl systems, respectively. Thus, the overall interaction between the two fragments becomes energetically favorable by −2.28 and −3.20 eV. Taking the preparation energies of 3.39 and 3.74 eV into account gives the final transition state energies of 18.6 and 12.4 kcal/mol for the acid-catalyzed *N*-alkyl and *N*-aryl imines. In summary, the energy decomposition shows that the main driving force for lowering the transition state energy is indeed elec-

(69) We use the energy unit eV in addition to kcal/mol to avoid nonintuitively large numerical values that would be required for for the Ziegler-Rauk terms.

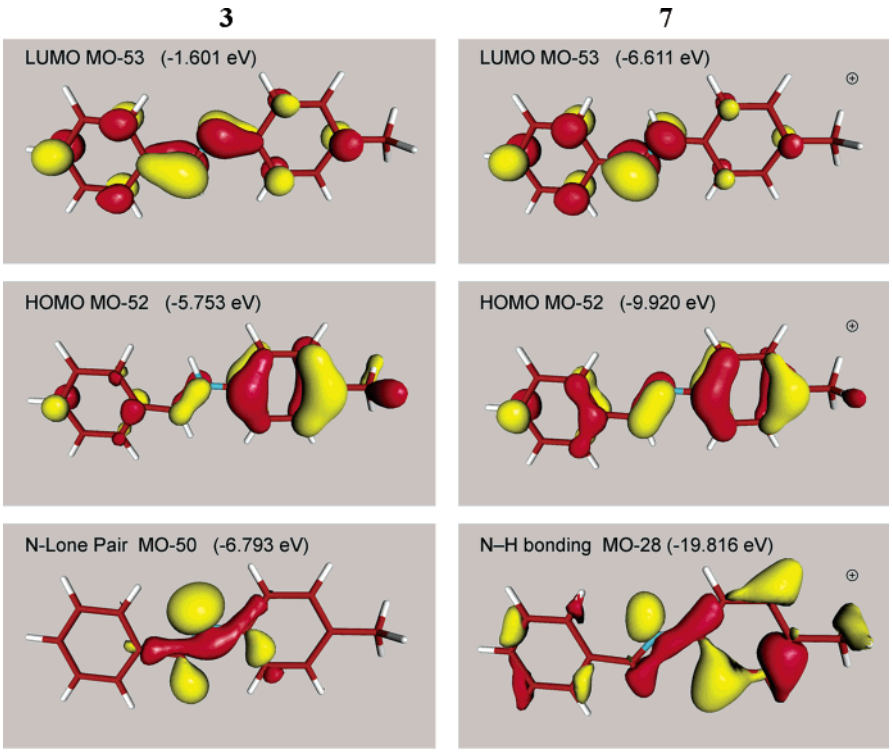

FIGURE 7. Isosurface plots (isodensity value = 0.05 au) of the most important molecular orbitals.

TABLE 5. Ziegler−Rauk Energy Decomposition of Activation Energies Referenced to the Noninteracting Monomers; All Energies Given in eV

	ΔE_{Prep}	ΔE_{Pauli}	$\Delta E_{\text{el-st}}$	$\Delta E_{\text{non-orb}}$[a]	$\Delta E_{\text{orb-int}}$	ΔE_{int}	$\Delta E^{\ddagger}$
			Uncatalyzed				
N-alkyl	0.640/0.644	9.170	−4.300	4.870	−3.435	1.435	2.719
N-aryl	0.634/0.464	8.964	−4.248	4.716	−3.528	1.188	2.286
			H(+)-Catalyzed				
N-alkyl	2.472[b]/0.920[c]	17.002	−7.531	9.471	−12.056	−2.585	0.807
N-aryl	2.671[b]/1.070[c]	17.636	−8.043	9.593	−12.797	−3.204	0.538

[a] $\Delta E_{\text{non-orb}}$ is defined as $\Delta E_{\text{Pauli}} + \Delta E_{\text{el-st}}$ and represents the total nonorbital contribution to the interaction of the fragments. [b] Preparation energy for the protonated iminium ion partner. [c] Preparation energy for the unprotonated imine partner.

tronic in nature with nonorbital interactions (Pauli + electrostatic) only playing a minor role.

Figure 8 shows the two most important MOs that promote intermolecular N−C bond, which is essentially formed to a full extend in the new asynchronous reaction path at the transition state. They are intuitively recognized as the transformations of the original π-orbitals, which have become significantly distorted to accommodate the new structural arrangement. Interestingly, the isosurface plots do not indicate that the 1s orbital of the proton participates in these MOs, indicating that the electronic effect of the protonation is not direct. Thus, there is nothing special about the electronic interaction of the proton with the imine moiety and attack by any Lewis acid at the imine-N position should give rise to catalytic behavior. Furthermore, the strong coupling of the MOs shown in Figure 8 with the σ-subspace of the aromatic substituents, as indicated by notably large amplitudes of the MOs in the aromatic rings, suggest that substitutions of the aromatic ring with electron-withdrawing substituents should destabilize the C−N bond formation process and thus increase the transition state energy, whereas electron-donating substituents on the aromatic rings will have the reverse effect. Strategies for exploiting this electronic feature are currently being explored both experimentally and computationally in our laboratories.

Conclusions

We explored the energetic and mechanistic features of the imine metathesis reaction. In comparison to olefin metathesis, substitution of $=CR_2$ with $=NR$ introduces a number of features that would appear to favor [2 + 2] addition of reactants, such as polarization of the π-electron cloud and breaking of the symmetry. Unfortunately, these features are inadequate for overcoming the significant barriers to reaction. However, the availability of a lone pair on nitrogen opens up new avenues for controlling the reaction. Protonation of the nitrogen lone pair on one of the two imine reactants dramatically reduces the activation energy for the reaction to the point that it becomes thermally accessible at modestly elevated temperatures.

In terms of electronic structure, the electrostatic force created by the proton reduces the energies of the imine molecular orbitals such that the LUMO of the iminium cation is lower in energy than the HOMO of the unpro-

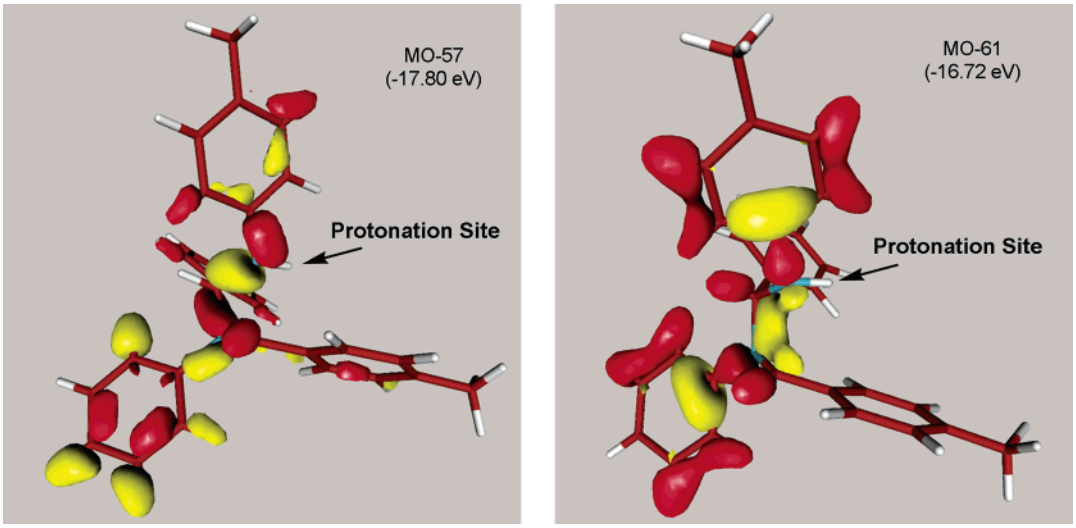

FIGURE 8. Isosurface plots (isodensity value = 0.05 au) of the two MOs promoting the intermolecular C−N bond formation at the transition state.

tonated imine. This shift in energy levels and the intrinsic distortions of the orbital shapes that accompany such shifts provide the driving force to deform the metathesis partners and allow a formerly symmetry forbidden process to occur. An interesting *N*-substituent effect is also relevant. When *N*-aryl groups are present the activation energies are significantly reduced compared to *N*-alkyl groups. The effect can be traced to stabilizing resonance effects in the transition state. The accelerating effect of *N*-aryl groups is somewhat muted when acid catalysis is used, since the protonation of the nitrogen disrupts some of the stabilization through resonance, but is still significant. Another *N*-substituent effect is observed from the energy decomposition. When more electron-donating *N*-aryl groups are compared to phenyl, the preparation energy is significantly higher. This is due to the destabilizing effect of electron donation to an already negatively polarized nitrogen center.

This work illuminated a number of key features of imine metathesis that are likely to be highly relevant to other metathesis processes. Asynchronous bond formation emerges as an effective way to "finance" bond breaking by returning energy via bond formation earlier in the reaction. The result is that although the same amount of energy is used to break bonds and the same amount of energy is returned through bond formation, having some of the energy released by bond formation returned sooner allows it to be invested back into bond breaking, thus reducing the amount of external energy that needs to be supplied to the system. This is the essential feature of the acid-catalyzed reaction that leads to the reduction of the activation energy. Furthermore, molecular orbital analyses revealed that the electronic features promoting the catalysis should in principle be also reproducible by any Lewis acidic additive that can polarize the nitrogen lone pair of the imine functionality.

Acknowledgment. This research was supported by Indiana University-Bloomington and the NSF (CHE-0091400 to T.Y.M.). Computational resources were provided by the NSF (0116050 and CDA-9601632 to Indiana University).

Supporting Information Available: A discussion of a comparative study involving highly simplified prototype imines at MP2 level of theory, free energy profiles, additional details, coordinates for optimized geometries of all calculations reported herein, calculated vibrational frequencies of all systems, and itemized energies. This material is available free of charge via the Internet at http://pubs.acs.org.

JO049250E